

Correlation between artificial intelligence-enabled electrocardiogram and echocardiographic features in aortic stenosis

Saki Ito ¹, Michal Cohen-Shelly^{1,2}, Zachi I. Attia ¹, Eunjung Lee¹, Paul A. Friedman¹, Vuyisile T. Nkomo¹, Hector I. Michelena¹, Peter A. Noseworthy ¹, Francisco Lopez-Jimenez ¹, and Jae K. Oh^{1,*}

¹Department of Cardiovascular Diseases, Mayo Clinic, 200 First Street SW Rochester, MN 55905, USA; and ²Department of Cardiology, Sheba Medical Center, Tel Hashomer, Israel

Received 6 July 2022; revised 25 November 2022; accepted 6 February 2023; online publish-ahead-of-print 8 February 2023

Aims

An artificial intelligence-enabled electrocardiogram (AI-ECG) is a promising tool to detect patients with aortic stenosis (AS) before developing symptoms. However, functional, structural, or haemodynamic components reflected in AI-ECG responsible for its detection are unknown.

Methods and results

The AI-ECG model that was developed at Mayo Clinic using a convolutional neural network to identify patients with moderate–severe AS was applied. In patients used as the testing group, the correlation between the AI-ECG probability of AS and echocardiographic parameters was investigated. This study included 102 926 patients (63.0 ± 16.3 years, 52% male), and 28 464 (27.7%) were identified as AS positive by AI-ECG. Older age, atrial fibrillation, hypertension, diabetes, coronary artery disease, and heart failure were more common in the positive AI-ECG group than in the negative group ($P < 0.001$). The AI-ECG was correlated with aortic valve area ($\rho = -0.48$, $R^2 = 0.20$), peak velocity ($\rho = 0.22$, $R^2 = 0.08$), and mean pressure gradient ($\rho = 0.35$, $R^2 = 0.08$). The AI-ECG also correlated with left ventricular (LV) mass index ($\rho = 0.36$, $R^2 = 0.13$), E/e' ($\rho = 0.36$, $R^2 = 0.12$), and left atrium volume index ($\rho = 0.42$, $R^2 = 0.12$). Neither LV ejection fraction nor stroke volume index had a significant correlation with the AI-ECG. Age correlated with the AI-ECG ($\rho = 0.46$, $R^2 = 0.22$) and its correlation with echocardiography parameters was similar to that of the AI-ECG.

Conclusion

A combination of AS severity, diastolic dysfunction, and LV hypertrophy is reflected in the AI-ECG to detect AS. There seems to be a gradation of the cardiac anatomical/functional features in the model and its identification process of AS is multifactorial.

* Corresponding author. Tel: +507 266 1376, Fax: +507 266 9142, Email: oh.jae@mayo.edu

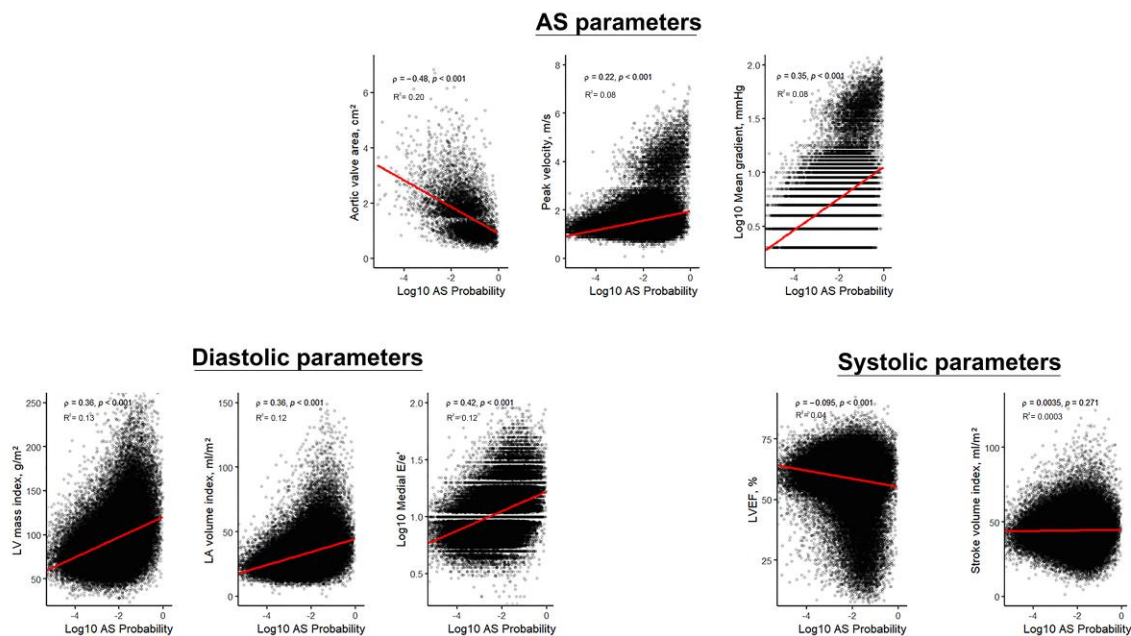
© The Author(s) 2023. Published by Oxford University Press on behalf of the European Society of Cardiology.

This is an Open Access article distributed under the terms of the Creative Commons Attribution-NonCommercial License (<https://creativecommons.org/licenses/by-nc/4.0/>), which permits non-commercial re-use, distribution, and reproduction in any medium, provided the original work is properly cited. For commercial re-use, please contact journals.permissions@oup.com

Graphical Abstract

Functional, structural, and hemodynamic components reflected in AI-ECG responsible for AS detection

- 1) The AI-ECG is correlated with AS severity
- 2) The AI-ECG is correlated with LV mass and diastolic dysfunction parameters (LA volume index and E/e')
- 3) The AI-ECG does not correlate with LVEF or SVI



Abbreviations: AI-ECG; artificial intelligence enabled electrocardiogram, AS; aortic stenosis, LVEF; left ventricular ejection fraction, LA; left atrium, SVI; stroke volume index

Functional, structural, and haemodynamic components reflected in artificial intelligence-enabled electrocardiogram (AI-ECG) for aortic stenosis (AS) are summarized.

Keywords

AI • Convolutional neural network • ECG • Aortic stenosis

Introduction

Recently, various artificial intelligence (AI) models have been developed for aortic stenosis (AS). The AI-enabled electrocardiogram (AI-ECG) models to identify patients with AS have been developed.^{1–3} The chest radiographs are also used for building the AI model for detecting patients with AS.⁴ By using AI models, the potential sex-specific gene sets that can achieve good predictability of valvular calcification have been also reported.⁵ The AI models are beneficial to patient identification and the characterization of AS.

Earlier detection of patients with AS even before developing symptomatic severe AS is becoming important with increasing evidence that asymptomatic patients with severe AS may benefit from aortic valve replacement (AVR).⁶ Moreover, some symptomatic patients with severe AS present too late to have optimal therapeutic results from AVR. There has been growing interest in the potential benefit of earlier AVR because of unfavourable survival outcomes in patients with moderate AS.^{7–10} The AI-ECG model that our group recently developed using a convolutional neural network (CNN) to identify patients with moderate-to-severe AS from the Mayo Clinic database is thus expected to play an important role in screening AS and improving

the management.¹ Its excellent ability has been demonstrated [area under the curve (AUC): 0.85]¹; however, specific functional, structural, and haemodynamic characteristics of AS reflected in the AI-ECG model have not been delineated. Changes in the QRS complex configuration on electrocardiogram (ECG) due to left ventricle (LV) hypertrophy in response to AS (e.g. increased R wave amplitude or increased S wave depth) were thought to be what identifies AS patients by AI-ECG, but the segment between the T and P wave has been reported to be most extensively utilized.^{1–3}

In this study, we investigated how AI-ECG probability for AS correlates with 2-dimensional and Doppler echocardiographic parameters to assess the impact of the functional, structural, and haemodynamic status of AS in the genesis of characteristic ECG patterns recognised by AI. This knowledge will improve our understanding of false positive and negative finding of AI-ECG, consequently a better detection of patients with AS.

Methods

In this study, testing data from the Mayo Clinic dataset between January 1989 and September 2019 which was previously used for developing the

AI-ECG model for identifying patients with moderate or severe AS were applied.¹ Details of the study design have been previously published.¹ Briefly, adults (age ≥ 18 years) who had available both an echocardiography and an ECG performed within 180 days were identified and the AI-ECG model was developed using CNN. The total number was 258 607; training was in 129 788 (50%), validation in 25 893 (10%), and testing in 102 926 (40%), respectively. AS severity was defined along with the current guidelines using echocardiography.^{11,12} If one of the following echocardiography criteria was met, diagnosis of moderate or severe AS was given: peak velocity ≥ 3.0 m/s, mean pressure gradient (MG) ≥ 20 mmHg, dimensionless velocity index (DVI) ≤ 0.35 , or aortic valve area (AVA) ≤ 1.5 cm². Exclusion criteria included previous cardiac surgery or permanent pacemaker implantation. The threshold of the AI-ECG model for the probability of classifying an ECG into positive and negative AS screens which was established as 0.0243 by Youden index in the validation set in the model training process was used. In this *post hoc* study, we investigate the correlation between the AI-ECG probability of moderate or severe AS and echocardiography parameters.

Patients' demographics were identified using ICD-9 and -10 codes. The Institutional Review Board approved the study and patients who had authorised research participation were involved.

Echocardiography

All echocardiography data were retrieved using the Mayo Clinic Unified Data Platform. AVA was calculated by the continuity equation.¹³ Peak velocity and MG were acquired by continuous wave Doppler and obtained from all available views, and the highest value was used.^{12,14} DVI was a ratio between left ventricular outflow tract (LVOT) and AV velocity time integral (VTI).¹⁵ LV ejection fraction (LVEF) was calculated by the modified Simpson or the modified Quinones method.¹⁶ Stroke volume index (SVI) was calculated as LVOT VTI \times cross-sectional area at LVOT and indexed for body surface area (BSA).¹⁶ Early (E) transmitral filling peak velocity, septal mitral e' were measured in a standard fashion.¹⁷ Left ventricular mass index (LVMI) was calculated by the Devereux formula and indexed for BSA.¹⁶ Left atrium volume index (LAVI) was calculated using the area-length method, method of disks, or prolate ellipse method and indexed for BSA.¹⁶

Statistical methods

Continuous variables were summarised as a mean \pm standard deviation or median (interquartile range) when appropriate. Categorical variables were summarised using frequency and percentage. For continuous variables, groups were compared using two-sample t-test. Binary data were compared with a χ^2 test. The correlation between the AI-ECG probability of AS and echocardiography parameters was assessed using a linear regression model. Spearman's correlation coefficient (ρ) and R^2 were reported. Decadic logarithm (log 10) transformation was applied when data were non-normal. A two-tailed P value < 0.05 was considered significant; however, its interpretation was carefully and comprehensively made because of the large sample size. Analyses were performed using R version 3.6.2 (The R Foundation, Vienna, Austria).

Results

Of a total of 102 926 patients, $n = 28 464$ (28%) were identified as AS positive according to the established threshold in the AI-ECG model (≥ 0.0243).¹ In those with AI-ECG positive ($n = 28 464$), patients with moderate AS were 830 (3%) and severe AS were 2615 (8%), respectively (Table 1). In those with AI-ECG negative ($n = 74 462$), AS was mild in 4648 (6%) patients and none AS was in 68 976 (93%) patients. These findings were consistent with our previous report; low positive predictive value at 11% and high negative predictive value at 99% were due to the low prevalence of the disease in this cohort (4%).¹ The prevalence of positive AI-ECG in each group of AS severity diagnosed by echocardiography was followed; none AS 24%, mild AS 44%, moderate AS 68%, and severe AS 83%, respectively (see Supplementary material online, Table S1). AS with low-flow (SVI < 35 mL/m²) was present in 13.9%

of the severe AS group and 9.7% of the moderate AS group (see Supplementary material online, Table S1).

Patient's clinical characteristics, echocardiography, and ECG data are presented in Table 1. Mean age was 63.0 ± 16.3 years and 52% was men. Compared to patients with AI-ECG negative, patients with AI-ECG positive were 11 years older and male sex was more common ($P < 0.001$ for both). Patients with AI-ECG positive had a higher prevalence of atrial fibrillation/flutter, hypertension, diabetes mellitus, congestive heart failure (CHF), myocardial infarction, coronary artery disease, peripheral artery disease, cerebrovascular disease, renal disease, and chronic pulmonary disease ($P < 0.001$ for all). In the AI-ECG positive group, patients with CHF ($n = 8180$) had LVEF of < 40 , 40–50, and $> 50\%$ in 32.9% ($n = 2691$), 16.7% ($n = 1364$), and 50.4% ($n = 4125$), respectively, indicating heart failure of preserved ejection fraction (HFpEF) was the most common in this cohort. The prevalence of decreased SVI (< 35 mL/m²) was higher in patients with CHF compared to those without CHF [31.8% ($n = 2516$) vs. 13.6% ($n = 2648$), $P < 0.001$].

Artificial intelligence-enabled electrocardiogram probability and echocardiographic parameters

Aortic valve area was similar between the AI-ECG positive and negative group (Table 1, 3.07 ± 63.22 vs. 3.07 ± 2.44 cm², $P < 0.001$); however, patients with positive AI-ECG had extremely wide standard deviation. This was also the case for DVI. Peak velocity and MG were higher in the AI-ECG positive group compared to the negative group ($P < 0.001$). LVEF was lower in the AI-ECG positive group than the negative group, but the difference was not significant (56.7 ± 12.8 vs. $59.8 \pm 9.2\%$, $P < 0.001$). Stroke volume (SV) and SVI were equivalent between the groups. LVMI was larger in the positive group than in the negative group ($P < 0.001$). Advanced diastolic dysfunction was more common in the AI-ECG positive group compared to the negative group; patients with the AI-ECG positive had higher medial E/e' and a larger LVMI and LAVI ($P < 0.001$).

A summary of our findings (Graphical Abstract) and the correlation between AI-ECG probability and echocardiography parameters (Figure 1) are shown, respectively. There was a negative correlation between AI-ECG and AVA ($\rho = -0.48$, $R^2 = 0.20$, $P < 0.001$) and a positive correlation for peak velocity ($\rho = 0.22$, $R^2 = 0.08$, $P < 0.001$) as well as MG ($\rho = 0.35$, $R^2 = 0.08$, $P < 0.001$). Due to the large sample size, the correlation between AI-ECG probability and LVEF ($\rho = -0.095$, $R^2 = 0.04$, $P < 0.001$) was thought to be insignificant. There was no significant correlation between AI-ECG probability and SVI ($\rho = 0.0035$, $R^2 = 0.0003$, $P = 0.271$). The correlation between AI-ECG and LV systolic parameters was shown to be poor. For diastolic parameters, there was a positive correlation between AI-ECG and LVMI ($\rho = 0.36$, $R^2 = 0.13$, $P < 0.001$), E/e' ($\rho = 0.36$, $R^2 = 0.12$, $P < 0.001$), and LAVI ($\rho = 0.42$, $R^2 = 0.12$, $P < 0.001$), respectively.

Of note, the impact of cardiomyopathies on the correlation between the AI-ECG and LVMI was thought to be minimal since the number of patients with cardiomyopathies (e.g. hypertrophic cardiomyopathy, Fabry disease, amyloidosis) was small (see Supplementary material online, Table S2).

Artificial intelligence-enabled electrocardiogram probability and electrocardiogram parameters

The AI-ECG positive group had longer PR-interval, QRS, and QT (QTc) (Table 1). There was a positive correlation between AI-ECG and QRS duration ($\rho = 0.25$, $R^2 = 0.08$, $P < 0.001$), PR interval ($\rho = 0.25$, $R^2 = 0.03$, $P < 0.001$), and QTc ($\rho = 0.23$, $R^2 = 0.05$, $P < 0.001$) (Figure 2). However, these correlations were shown to be weak.

Table 1 Clinical, echocardiography, and electrocardiogram characteristics

	Overall (n = 102 926)	AI-ECG positive (n = 28 464)	AI-ECG negative (n = 74 462)	P
Age, years	63.0 ± 16.3	71.3 ± 13.4	59.8 ± 16.2	<0.001
Male sex, (%)	53 938 (52%)	16 386 (58%)	37 552 (50%)	<0.001
Body surface area, m ²	1.95 ± 0.27	1.94 ± 0.27	1.95 ± 0.27	<0.001
Aortic stenosis severity diagnosed by echocardiography				<0.001
None	90 763 (88%)	21 787 (77%)	68 976 (93%)	
Mild	8330 (8%)	3682 (13%)	4648 (6%)	
Moderate	1225 (1%)	830 (3%)	395 (1%)	
Severe	2608 (3%)	2165 (8%)	443 (1%)	
Clinical characteristics (%)				
Bicuspid aortic valve	2087 (2%)	821 (3%)	1266 (2%)	<0.001
Atrial fibrillation/flutter	10 760 (11%)	5068 (18%)	5692 (8%)	<0.001
Hypertension	50 486 (49%)	18 405 (65%)	32 081 (43%)	<0.001
Diabetes mellitus	18 186 (17.7%)	6951 (24.4%)	11 235 (15.1%)	<0.001
Congestive heart failure	18 531 (18.0%)	8180 (28.7%)	10 351 (13.9%)	<0.001
Myocardial infarction	9843 (10%)	3700 (13%)	6143 (8%)	<0.001
Coronary artery disease	27 148 (26%)	10 616 (37%)	16 532 (22%)	<0.001
Peripheral artery disease	16 134 (16%)	6447 (23%)	9687 (13%)	<0.001
Cerebrovascular disease	11 879 (12%)	4969 (18%)	6910 (9%)	<0.001
Renal disease	12 394 (12.0%)	5260 (18.5%)	7134 (9.6%)	<0.001
Chronic pulmonary disease	20 932 (20%)	6832 (24%)	14 100 (19%)	<0.001
Echocardiography				
Aortic valve area, cm ²	3.07 ± 33.56	3.07 ± 63.22	3.07 ± 2.44	0.999
Peak velocity, m/s	1.53 ± 0.61	1.78 ± 0.90	1.43 ± 0.40	<0.001
Mean pressure gradient, mmHg	8.39 ± 10.99	13.58 ± 16.18	5.87 ± 5.71	<0.001
Dimensionless velocity index	0.76 ± 0.63	0.69 ± 0.81	0.79 ± 0.54	<0.001
LV ejection fraction, %	58.9 ± 10.4	56.7 ± 12.8	59.8 ± 9.2	<0.001
Stroke volume, mL	86.1 ± 22.3	86.1 ± 23.5	86.1 ± 21.8	0.94
Indexed stroke volume, mL/m ²	44.3 ± 10.4	44.6 ± 11.5	44.2 ± 9.9	<0.001
Indexed stroke volume, mL/m ² < 35 mL/m ² (%)	16 548 (16.7%)	5164 (18.8%)	11 384 (15.9%)	<0.001
Medial E/e'	12.0 ± 15.5	15.1 ± 10.2	10.9 ± 16.9	<0.001 ^a
LA volume index, mL/m ²	33.6 ± 13.2	39.5 ± 15.4	31.3 ± 11.4	<0.001
LV mass index, g/m ²	95.4 ± 28.3	109.3 ± 33.1	90.1 ± 24.3	<0.001
ECG				
Ventricular rate, b.p.m.	75.0 ± 18.9	76.2 ± 17.6	74.5 ± 19.3	<0.001
PR interval	162.5 ± 40.2	170.1 ± 54.0	159.9 ± 33.8	<0.001
QRS duration	96.4 ± 20.3	105.0 ± 25.5	93.1 ± 16.7	<0.001
QT	399.3 ± 46.1	403.6 ± 46.3	397.7 ± 45.9	<0.001
QTc	437.6 ± 33.6	447.0 ± 36.2	434.0 ± 31.8	<0.001
P axis	47.6 ± 27.4	46.5 ± 30.5	47.9 ± 26.2	<0.001
R axis	22.0 ± 45.3	12.8 ± 52.5	25.5 ± 41.7	<0.001
T axis	47.0 ± 47.6	57.5 ± 60.6	43.0 ± 40.8	<0.001

AI-ECG, artificial intelligence-enabled electrocardiogram; ECG, electrocardiogram; E/e', ratio between mitral inflow early diastolic velocity and medial mitral annular early diastolic velocity; LA, left atrium; LV, left ventricle.

^aComparison is performed after applying decadic logarithm transformation (log 10).

Artificial intelligence-enabled electrocardiogram probability and age

There was a positive correlation between AI-ECG probability and age (Figure 3, $\rho = 0.46$, $R^2 = 0.22$, $P < 0.001$). Consistently, the prevalence of positive AI-ECG increased as age increased (Table 2, age < 60 years:

12.8%, 60–70 years: 25.2%, 70–80 years: 37.0%, ≥ 80 years: 53.4%; $P < 0.001$). As age increased, the prevalence of moderate and severe AS diagnosed by echocardiography also increased (Table 2, e.g. severe AS: age < 60 years: 0.6%, 60–70 years: 1.7%, 70–80 years: 3.4%, ≥ 80 years: 7.3%). The prevalence of comorbid conditions increased as age increased, inversely, bicuspid AV became less common ($P < 0.001$).

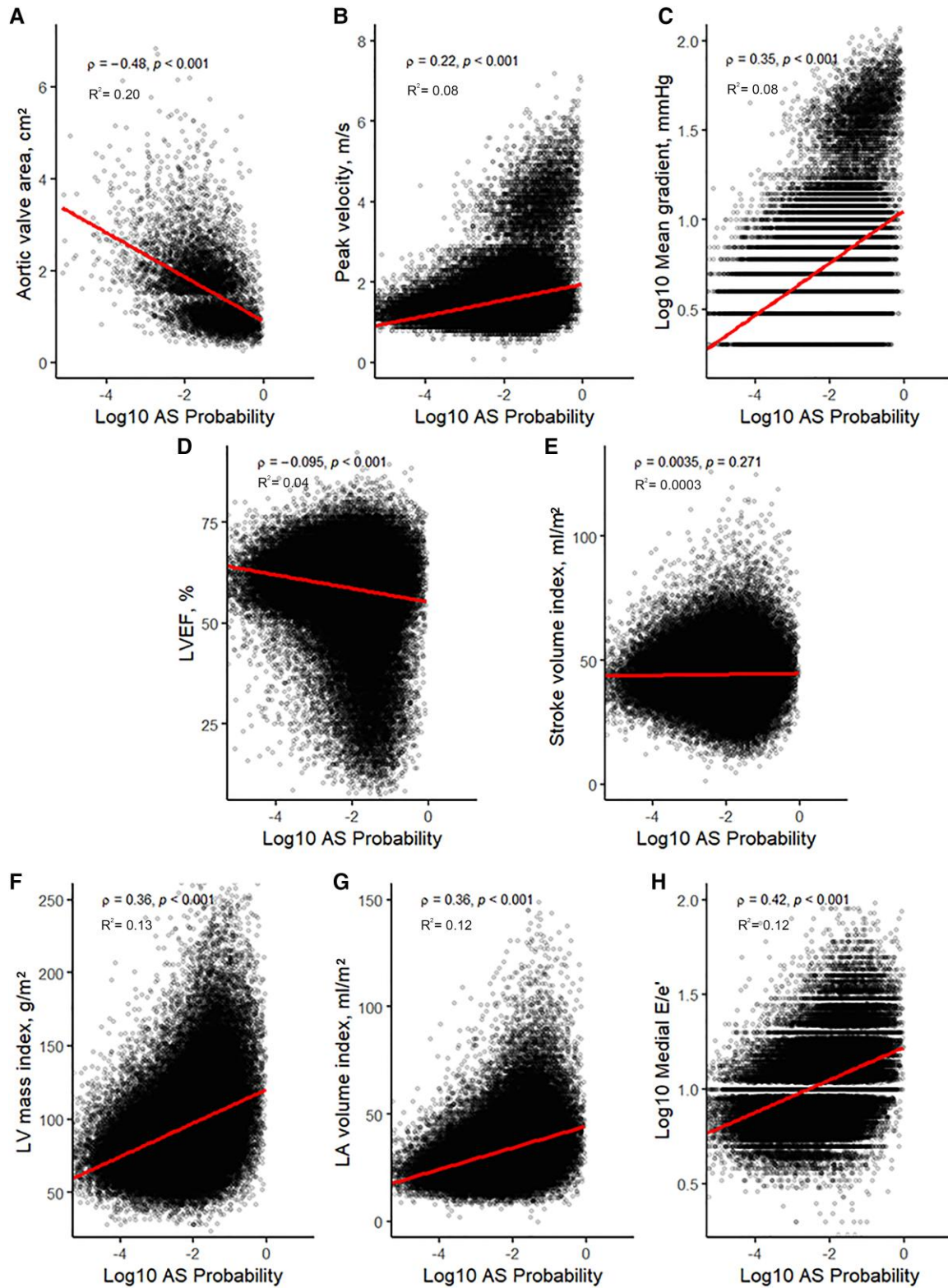
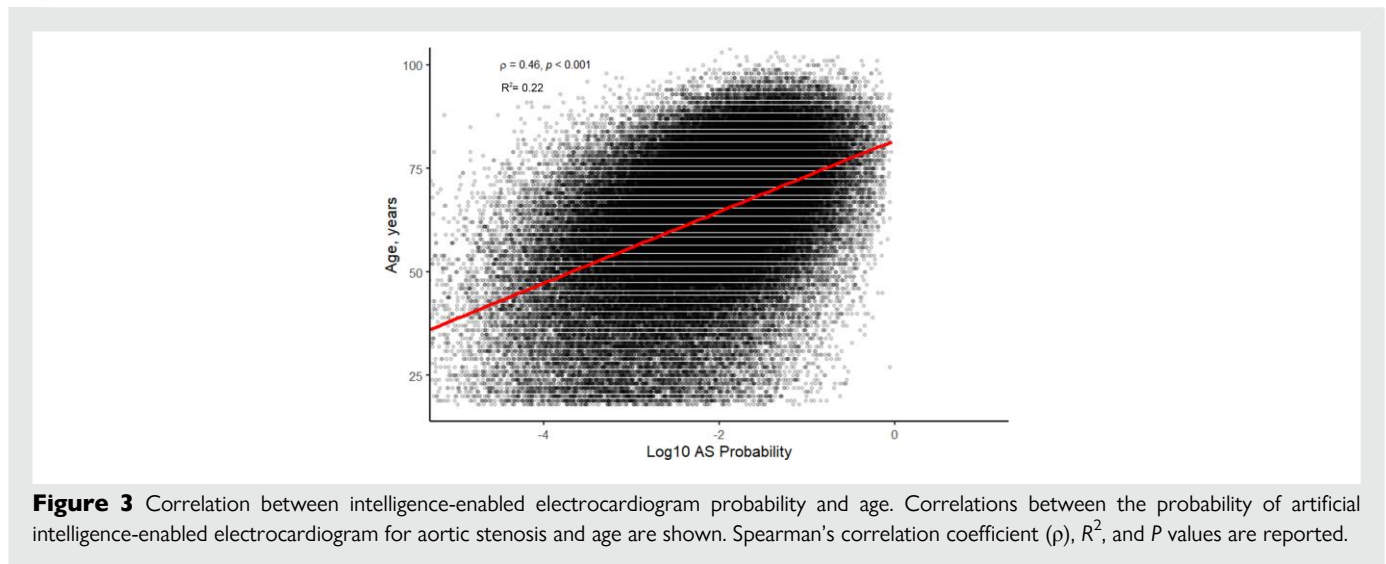
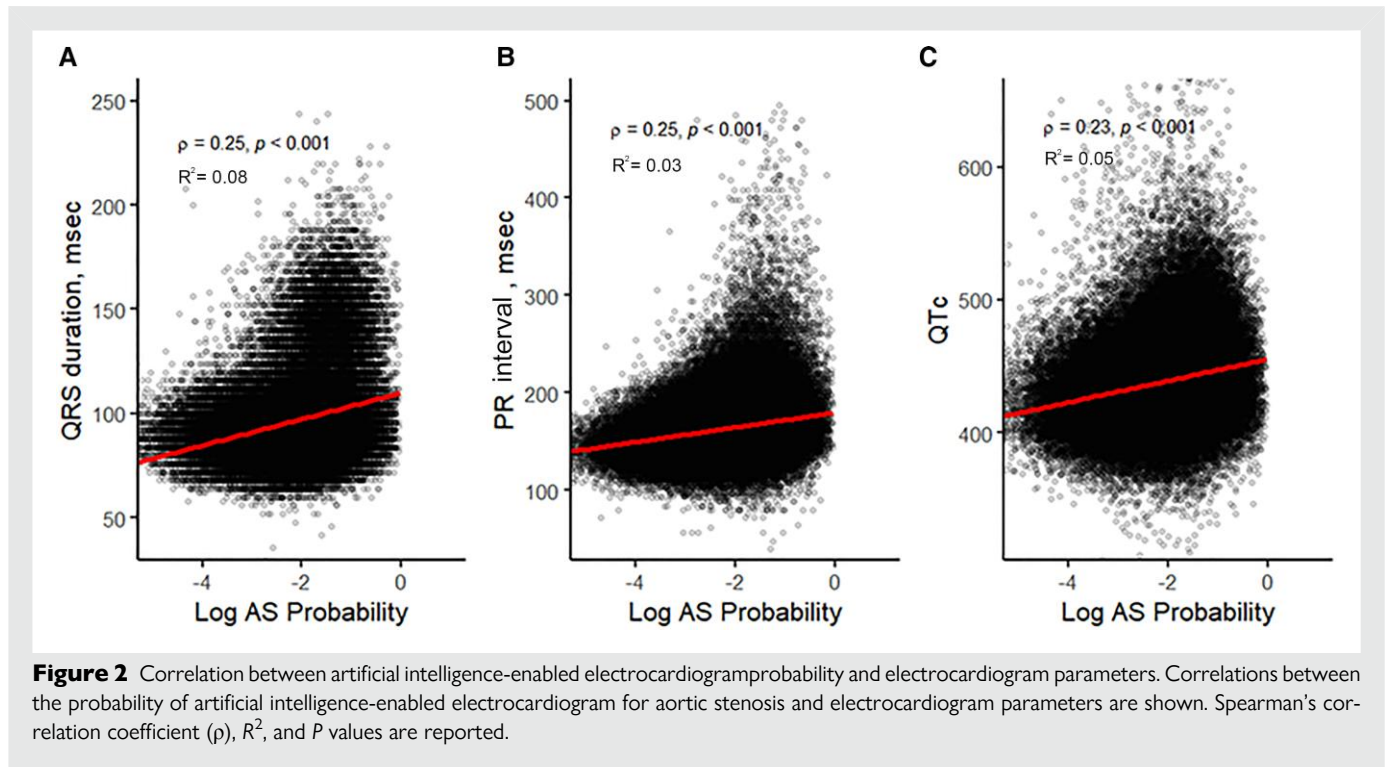


Figure 1 Correlation between artificial intelligence-enabled electrocardiogram probability and echocardiography parameters. Correlations between the probability of artificial intelligence-enabled electrocardiogram for aortic stenosis and echocardiography parameters using linear regression model are shown. Spearman's correlation coefficient (ρ), R^2 , and P values are reported. LVEF, left ventricular ejection fraction; LA, left atrium.



Furthermore, as age increased, AS severity increased (AVA, peak velocity, and MG) and diastolic function deteriorated (increase in E/e' , LAVI, and LVMI) ($P < 0.001$). Although statistical significance was present ($P < 0.001$), LVEF and SVI were similar between the age groups.

The correlation between age and each echocardiography parameter was similar to that of the AI-ECG probability (Figure 4). A negative correlation between age and AVA ($\rho = -0.3$, $R^2 = 0.14$, $P < 0.001$) and a positive correlation for peak velocity ($\rho = 0.2$, $R^2 = 0.05$, $P < 0.001$) as well as MG ($\rho = 0.26$, $R^2 = 0.05$, $P < 0.001$) were seen. The correlation was not significant for LVEF ($P = 0.882$) and not relevant for SVI ($\rho = 0.055$, $R^2 = 0.0003$, $P < 0.001$). Age had positive correlation with LVMI ($\rho = 0.04$, $R^2 = 0.22$, $P < 0.001$), LAVI ($\rho = 0.38$, $R^2 = 0.12$, $P < 0.001$), and LAVI ($\rho = 0.43$, $R^2 = 0.12$, $P < 0.001$), respectively.

However, even after adjusting for age and sex, the AI-ECG probability significantly correlated with AS severity (AVA, peak velocity, and MG) as well as diastolic parameters (E/e' , LAVI, and LVMI) ($P < 0.001$ for all).

Discussion

This study found the following: (i) AI-ECG is positive in 68% of patients with moderate AS and 83% of those with severe AS, (ii) AI-ECG probability is positively correlated with AS severity and LVMI as well as LV diastolic parameters, (iii) age was one of the important determinants of the AI-ECG probability; this is mostly because that the prevalence of AS increased as age increased and the AI feature for AS overlaps with aging.

Table 2 Clinical, echocardiography, and electrocardiogram characteristics according to age

	Age < 60 (n = 38 237)	Age 60–70 (n = 24 970)	Age 70–80 (n = 24 077)	Age ≥ 80 (n = 15 642)	P
Age, years	45.7 ± 11.0	64.7 ± 2.9	74.3 ± 2.9	85.0 ± 4.2	—
Male sex, (%)	18 803 (49.2%)	14 063 (56.3%)	13 294 (55.2%)	7778 (49.7%)	<0.001
Body surface area, m ²	1.98 ± 0.29	1.99 ± 0.27	1.93 ± 0.25	1.83 ± 0.23	<0.001
AI-ECG probability	0.118 ± 0.621	0.273 ± 0.966	0.494 ± 1.307	0.894 ± 1.732	<0.001
AI-ECG positive (%)	4912 (12.8%)	6296 (25.2%)	8898 (37.0%)	8358 (53.4%)	<0.001
Aortic stenosis severity diagnosed by echocardiography					<0.001
None	36 532 (95.5%)	22 590 (90.5%)	20 206 (83.9%)	11 435 (73.1%)	
Mild	1380 (3.6%)	1765 (7.1%)	2613 (10.9%)	2572 (16.4%)	
Moderate	97 (0.3%)	202 (0.8%)	438 (1.8%)	488 (3.1%)	
Severe	228 (0.6%)	413 (1.7%)	820 (3.4%)	1147 (7.3%)	
Clinical characteristics (%)					
Bicuspid aortic valve	1002 (2.6%)	584 (2.3%)	370 (1.5%)	131 (0.8%)	<0.001
Atrial fibrillation/flutter	1256 (3.3%)	2399 (9.6%)	3582 (14.9%)	3523 (22.5%)	<0.001
Hypertension	11 919 (31.2%)	12 870 (51.5%)	14 694 (61.0%)	11 003 (70.3%)	<0.001
Diabetes mellitus	4728 (12.4%)	5191 (20.8%)	5207 (21.6%)	3060 (19.6%)	<0.001
Congestive heart failure	4687 (12.3%)	4211 (16.9%)	4876 (20.3%)	4757 (30.4%)	<0.001
Myocardial infarction	2267 (5.9%)	2357 (9.4%)	2731 (11.3%)	2488 (15.9%)	<0.001
Coronary artery disease	5469 (14.3%)	7226 (28.9%)	8556 (35.5%)	5897 (37.7%)	<0.001
Peripheral artery disease	2897 (7.6%)	3795 (15.2%)	5168 (21.5%)	4274 (27.3%)	<0.001
Cerebrovascular disease	1941 (5.1%)	2532 (10.1%)	3699 (15.4%)	3707 (23.7%)	<0.001
Renal disease	3271 (8.6%)	2908 (11.6%)	3179 (13.2%)	3036 (19.4%)	<0.001
Chronic pulmonary disease	5929 (15.5%)	4946 (19.8%)	5762 (23.9%)	4295 (27.5%)	<0.001
Echocardiography					
Aortic valve area, cm ²	2.20 ± 1.08	1.74 ± 0.79	1.55 ± 0.68	1.37 ± 0.66	<0.001
Peak velocity, m/s	1.39 ± 0.394	1.51 ± 0.54	1.61 ± 0.68	1.76 ± 0.86	<0.001
Mean pressure gradient, mmHg	5.63 ± 6.91	7.56 ± 9.71	9.52 ± 11.79	12.30 ± 14.65	<0.001
Dimensionless velocity index	0.80 ± 0.12	0.76 ± 0.14	0.71 ± 0.17	0.65 ± 0.20	<0.001
LV ejection fraction, %	59.3 ± 9.3	59.0 ± 10.6	58.9 ± 10.8	57.9 ± 11.7	<0.001
Stroke volume, mL	86.3 ± 22.4	88.2 ± 22.5	86.5 ± 22.0	81.5 ± 21.5	<0.001
Indexed stroke volume, mL/m ²	43.6 ± 9.8	44.4 ± 10.3	44.9 ± 10.6	44.8 ± 11.2	<0.001
Indexed stroke volume, mL/m ² < 35 mL/m ² (%)	6083 (16.5%)	3902 (16.3%)	3758 (16.2%)	2805 (18.6%)	<0.001
Medial E/e'	9.7 ± 4.6	11.9 ± 5.7	13.2 ± 6.2	15.7 ± 7.9	<0.001 ^a
LA volume index, mL/m ²	28.9 ± 10.5	33.6 ± 12.3	36.5 ± 13.5	41.3 ± 15.5	<0.001
LV mass index, g/m ²	89.4 ± 27.5	96.8 ± 28.1	99.0 ± 28.2	102.7 ± 29.9	<0.001
ECG					
Ventricular rate, b.p.m.	75.4 ± 18.7	74.6 ± 18.7	74.3 ± 18.8	75.7 ± 19.5	<0.001
PR interval	154.6 ± 28.9	162.9 ± 36.9	168.7 ± 46.7	175.2 ± 59.4	<0.001
QRS duration	92.9 ± 15.6	96.3 ± 19.9	98.8 ± 22.5	101.6 ± 24.9	<0.001
QT	393.5 ± 42.5	401.0 ± 45.7	403.0 ± 47.6	405.2 ± 51.1	<0.001
QTc	432.6 ± 31.8	438.3 ± 33.1	439.6 ± 34.1	445.5 ± 36.0	<0.001
P axis	46.9 ± 23.9	47.9 ± 26.9	48.1 ± 30.1	48.2 ± 32.4	<0.001
R axis	35.1 ± 39.9	19.6 ± 43.9	13.5 ± 45.7	7.0 ± 50.3	<0.001
T axis	42.2 ± 39.1	47.0 ± 46.9	50.1 ± 52.1	54.1 ± 57.8	<0.001

AI-ECG, artificial intelligence-enabled electrocardiogram; ECG, electrocardiogram; E/e', ratio between mitral inflow early diastolic velocity and medial mitral annular early diastolic velocity; LA, left atrium; LV, left ventricle.

^aComparison is performed after applying decadic logarithm transformation (log 10).

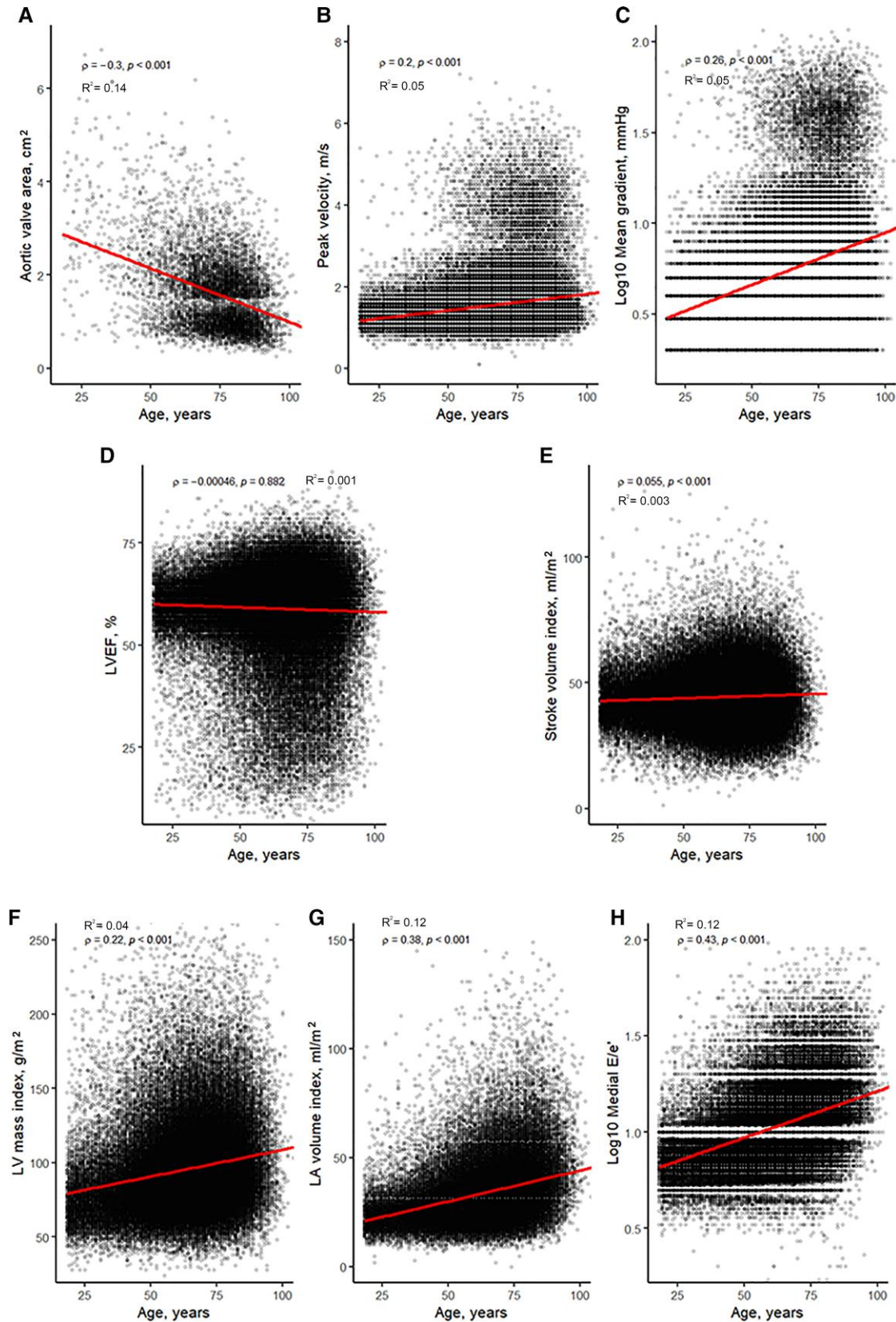


Figure 4 Correlation between age and echocardiography parameters. Correlations between age and echocardiography parameters are shown. Spearman's correlation coefficient (ρ), R^2 , and P values are reported. LVEF, left ventricular ejection fraction; LA, left atrium; LV, left ventricle.

Artificial intelligence-enabled electrocardiogram for detecting moderate or severe aortic stenosis

Because of better clinical outcomes following AVR in patients with asymptomatic severe AS⁶ and poor survival outcomes in patients with moderate AS,^{9,10} early detection of AS is becoming increasingly important. There has been growing interest in earlier AVR, and several clinical trials investigating the efficacy of transcatheter AVR (TAVR) in those with moderate AS are currently ongoing (TAVR UNLOAD: NCT02661451, PROGRESS; NCT04889872, EXPAND II; NCT05149755). Three AI-ECG models from the US, South Korea, and Japan have been developed for detecting patients with AS^{1–3} and have been expected to identify patients with AS even before developing symptomatic severe AS in the community as well as clinical practice. All models showed an excellent ability (AUC: 0.83–0.88)^{1–3}; however, it has not been clarified yet how to apply these models in practice. One of the important reasons for the difficulty for clinical application is its low positive predictive values (10.5–18.0%).^{1–3} This is mostly because the prevalence of patients with moderate to severe AS is low at approximately 3% even in those with age ≥ 75 years.^{18,19} To overcome this limitation, we are currently planning to investigate and develop the most effective way of using the AI-ECG in clinical practice as a screening tool by prospectively obtaining a point-of-care ultrasound in patients with positive AI-ECG for AS. Another important limitation would be that we do not know which features of AS are reflected in AI-ECG (black box). Without understanding its decision-making process, we may not be able to simply apply it to patients especially when we want to make a clinical decision. Our AI group at Mayo Clinic recently developed a set-up to understand which features of the ECG were used by human intelligence (medical expert) and by an AI model²⁰; however, the further effort remains necessary to understand the black box. In the current study, therefore, we studied how the AI-ECG probability of AS correlated with the cardiac structural, functional, and haemodynamic features assessed by echocardiography to understand the model identification process for AS.

In our AI model, the TP segment or U wave was found to be most heavily weighted for determining the presence of AS.¹ The AI-ECG model for AS from a Korean population showed that the initial area of the T wave in V2–V5 was the most important region.² The AI-ECG model from the Japanese population showed that the ST-T segment is weighted.³ Despite its significance, these findings are based on the representative ECG cases and the specific segments were identified by saliency maps or sensitivity maps, thus, it may not be generalised to all cases. Such a feature of ECG representing LV hypertrophy (e.g. increased R wave amplitude or increased S wave depth) was not identified as specific segments used by AI-ECG; however, it is possible that the models identify R or S wave, or even other ECG segments for determining the presence of AS. In fact, LV hypertrophy is a key adaptation mechanism against increased afterload in AS. There was a significant positive correlation between the AI-ECG probability and LVMI (Graphical Abstract, Figure 1). In addition, the AI-ECG probability positively correlated with AS severity (AVA, peak velocity, and MG). Based on the correlation coefficient (ρ), AVA and medial E/e' has a relatively strong correlation, and peak velocity, MG, LVMI, and LAVI had a moderate correlation with the AI-ECG probability. However, even for AVA, the R^2 was not so much high at 0.20 indicating that there might be significant diversity in its correlation with the AI-ECG. The AI-ECG positive group has longer PR-interval, QRS, and QTc indicating that those with AI-ECG positive may have advanced myocardial disease compared to those with AI-ECG negative. Based on these findings, we may be able to postulate that the AI model identifies a significant diversity of electrical disturbance that is associated with LV hypertrophy or myocardial disease that is induced by AS or other similar

cardiac conditions (e.g. high afterload associated with hypertension or atherosclerosis). In fact, in the AI-ECG positive group, patients were older and thus expected to have advanced atherosclerosis, and frequently had hypertension as well as peripheral artery disease compared to those with negative AI-ECG. Other comorbid conditions were also more frequent in those with AI-ECG positive than in the negative group. Comorbidities usually accelerate atrial stiffening resulting in a further increased LV afterload.^{21,22} These findings suggest the importance of systemic arterial compliance associated with high afterload in addition to AS severity in creating characteristic changes of AS in ECG.

Our study showed that advanced diastolic dysfunction such as higher E/e' and larger LAVI was associated with higher AI-ECG probability in addition to LVMI (Table 1, Graphical Abstract, Figure 1). Diastolic dysfunction or high LV filling pressure has been reported to be associated with dyspnoea as well as worse survival in patients with AS.^{23–25} In significant AS, LV hypertrophy occurs as a compensatory mechanism in an attempt to normalise wall stress in the setting of increased afterload.^{26–28} Reduced systemic arterial compliance has also been shown to induce LV hypertrophy and diastolic dysfunction in addition to AS.^{21,29} LV hypertrophy is a key adaptation mechanism against increased afterload in AS to preserve LV ejection performance; however, it is accompanied by increased resistance to diastolic filling and LA pressure increases as shown in our data.^{30,31}

The correlation between the AI-ECG probability and LVEF or SVI was not shown to be significant in the current study. Reduced LVEF (<50%) has been reported to be present approximately in 20% of patients with severe AS and its reduction has already started even before developing severe AS.³² Furthermore, impaired LVEF is associated with adverse survival outcomes in patients with AS.^{10,32} Despite its importance, the AI-ECG does not weight LV systolic function based on our data. Inconsistently, the prevalence of patients with CHF was higher in AI-ECG positive group compared to the negative group (Table 1, 28.7 vs. 13.9%), and 33% of patients with CHF had LVEF < 40%. According to these findings, the AI-ECG perhaps identifies electrical disturbance associated with systolic dysfunction in some cases. However, most importantly, patients with LVEF > 50% were present in 50% of those with CHF indicating significant importance of diastolic dysfunction (e.g. HFpEF) in this cohort. SVI is also an important factor in patients with AS. Its prognostic value has been well documented,^{33,34} and the SV reduction in progressive AS from moderate to severe AS is well described.³⁵ For our AI model, severe or moderate AS was defined using Doppler echocardiography parameters, and low-flow low-gradient AS is theoretically identified by the model. Patients with low-flow (SVI < 35 mL/m²) were present at 14% in the severe AS group and 10% in the moderate AS group, respectively (see Supplementary material online, Table S1). Low-flow status was much more common in patients with CHF than those without CHF (32 vs. 14%).

Artificial intelligence-enabled electrocardiogram probability and age

In the original manuscript,¹ we demonstrated that model performance increased when age and sex were added to the model (AUC: 0.85–0.87). Further analysis of stratifying based on the age groups, we demonstrated that the sensitivity gradually increased, and the specificity decreased as age increased.¹ Patients with positive AI-ECG were much older than the negative group and there was a correlation between the AI-ECG and age (Table 1, Figure 3). The correlation between the AI-ECG and echocardiography parameters was similar to that of age and echocardiography parameters (Figures 1 and 4). We believe this is because the prevalence of AS increased as age increased (Table 2), and the AI feature for AS overlaps with features associated with aging. Comorbidities such as hypertension and peripheral artery

disease that are associated with advanced atherosclerosis are more frequent in the older group of patients. These comorbidities are risk factors for AS itself but are also associated with increased high afterload in addition to AS.

It may be better to incorporate age, sex, and several medical conditions into the model to improve diagnostic accuracy; however, we aimed to develop the model as a stand-alone screening tool in the community that can be utilised for individuals who do not have available medical information.¹ To have better diagnostic accuracy, we are currently planning to incorporate several AI-ECG models that have been previously developed (e.g. LV systolic dysfunction, age and sex, silent atrial fibrillation, and hypertrophic cardiomyopathy).^{36–39}

Future directions

Although AS severity, LVMI, and diastolic function have a relatively strong correlation with the AI-ECG probability of AS, it is obvious that the model detects amalgam of several features associated with AS. Its identification for AS process is multifactorial and there seems to be a gradation of the cardiac anatomical/functional features and dysfunction in the model. It may be possible that AI-ECG recognises parameters yet to be identified at this time; therefore, further studies are warranted. Not infrequently, there is a discrepancy between AS severity based on its valvular haemodynamics and patients' symptoms or LV filling pressures. Therefore, it may be possible that AI-ECG can help us to identify patients who have AS-specific cardiac maladaptation and predict which patients can benefit most from AVR in the future.

Limitations

Since our model was developed from the Mayo Clinic database, we need to validate its generalizability in an external group. Additional testing of our AI-ECG in different races and different parts of the world is currently planned. However, as long as the purpose of the study is identifying echocardiographic features related to the AI-ECG probability, internal use should be sufficient. In this study, we aimed to demonstrate how the AI-ECG probability is correlated with each echocardiography parameter, thus, correlation coefficient and R^2 were important. However, in the majority of the linear regression models, the R^2 s were relatively low. These findings indicate that there might be significant diversity in the recognition process by the AI model but also suggest that the AI-ECG for AS has significant overlap with features associated with other conditions in the elderly.

Conclusions

Combined features from AS severity, LV hypertrophy, and diastolic dysfunction are reflected in the AI-ECG model to detect AS. There seems to be a gradation of the cardiac anatomical/functional features in the model and its identification process for AS is multifactorial. The prevalence of AS increased with aging, thus the AI feature for AS overlaps with cardiac conditions associated with aging.

Supplementary material

Supplementary material is available at *European Heart Journal – Digital Health*.

Funding

None declared.

Conflict of interest: J.K.O. serves as a consultant for Medtronic's valve projects. Z.I.A., E.L., P.A.F., P.A.N., F.L.-J., and J.K.O. have invented algorithms licensed to ANUMANA and may benefit from algorithm

commercialization via Mayo Clinic. H.I.M. serves as a consultant for Artivion and co-PI for PROACT Xa trial, and as a consultant for Biostable Science and Engineering Inc. The remaining authors have nothing to disclose.

Data availability

The data underlying this article will be shared on reasonable request to the corresponding author.

References

- Cohen-Shelly M, Attia ZI, Friedman PA, Ito S, Essayagh BA, Ko WY, et al. Electrocardiogram screening for aortic valve stenosis using artificial intelligence. *Eur Heart J* 2021;**42**:2885–2896.
- Kwon JM, Lee SY, Jeon KH, Lee Y, Kim KH, Park J, et al. Deep learning-based algorithm for detecting aortic stenosis using electrocardiography. *J Am Heart Assoc* 2020;**9**: e014717.
- Hata E, Seo C, Nakayama M, Iwasaki K, Ohkawauchi T, Ohya J. Classification of aortic stenosis using ECG by deep learning and its analysis using grad-CAM. *Annu Int Conf IEEE Eng Med Biol Soc* 2020;**2020**:1548–1551.
- Ueda D, Yamamoto A, Ehara S, Iwata S, Abo K, Walston SL, et al. Artificial intelligence-based detection of aortic stenosis from chest radiographs. *Eur Heart J Digit Health* 2022;**3**:20–28.
- Sarajlic P, Plunde O, Franco-Cereceda A, Back M. Artificial intelligence models reveal sex-specific gene expression in aortic valve calcification. *JACC Basic Transl Sci* 2021;**6**: 403–412.
- Kang DH, Park SJ, Lee SA, Lee S, Kim DH, Kim HK, et al. Early surgery or conservative care for asymptomatic aortic stenosis. *N Engl J Med* 2020;**382**:111–119.
- Delesalle G, Bohbot Y, Rusinaru D, Delpierre Q, Marechaux S, Tribouilloy C. Characteristics and prognosis of patients with moderate aortic stenosis and preserved left ventricular ejection fraction. *J Am Heart Assoc* 2019;**8**:e011036.
- van Gils L, Clavel MA, Vollema EM, Hahn RT, Spitzer E, Delgado V, et al. Prognostic implications of moderate aortic stenosis in patients with left ventricular systolic dysfunction. *J Am Coll Cardiol* 2017;**69**:2383–2392.
- Strange G, Stewart S, Celermajer D, Prior D, Scalia GM, Marwick T, et al. Poor long-term survival in patients with moderate aortic stenosis. *J Am Coll Cardiol* 2019;**74**: 1851–1863.
- Ito S, Miranda WR, Nkomo VT, Boler AN, Pislaru SV, Pellikka PA, et al. Prognostic risk stratification of patients with moderate aortic stenosis. *J Am Soc Echocardiogr* 2021;**34**: 248–256.
- Baumgartner H, Falk V, Bax JJ, De Bonis M, Hamm C, Holm PJ, et al. 2017 ESC/EACTS Guidelines for the management of valvular heart disease. *Eur Heart J* 2017;**38**: 2739–2791.
- Baumgartner H, Hung J, Bermejo J, Chambers JB, Edvardsen T, Goldstein S, et al. Recommendations on the echocardiographic assessment of aortic valve stenosis: a focused update from the European association of cardiovascular imaging and the American Society of Echocardiography. *J Am Soc Echocardiogr* 2017;**30**:372–392.
- Baumgartner H, Hung J, Bermejo J, Chambers JB, Evangelista A, Griffin BP, et al. Echocardiographic assessment of valve stenosis: EAE/ASE recommendations for clinical practice. *J Am Soc Echocardiogr* 2009;**22**:1–23.
- Thaden JJ, Nkomo VT, Lee KJ, Oh JK. Doppler imaging in aortic stenosis: the importance of the nonapical imaging windows to determine severity in a contemporary cohort. *J Am Soc Echocardiogr* 2015;**28**:780–785.
- Oh JK, Taliencio CP, Holmes DR Jr, Reeder GS, Bailey KR, Seward JB, et al. Prediction of the severity of aortic stenosis by Doppler aortic valve area determination: prospective Doppler-catheterization correlation in 100 patients. *J Am Coll Cardiol* 1988;**11**: 1227–1234.
- Lang RM, Badano LP, Mor-Avi V, Afilalo J, Armstrong A, Ernande L, et al. Recommendations for cardiac chamber quantification by echocardiography in adults: an update from the American Society of Echocardiography and the European Association of Cardiovascular Imaging. *J Am Soc Echocardiogr* 2015;**28**:1–39 e14.
- Nagueh SF, Smiseth OA, Appleton CP, Byrd BF III, Dokainish H, Edvardsen T, et al. Recommendations for the evaluation of left ventricular diastolic function by echocardiography: an update from the American Society of Echocardiography and the European Association of Cardiovascular Imaging. *J Am Soc Echocardiogr* 2016;**29**:277–314.
- Nkomo VT, Gardin JM, Skelton TN, Gottdiener JS, Scott CG, Enriquez-Sarano M. Burden of valvular heart diseases: a population-based study. *Lancet* 2006;**368**: 1005–1011.
- Osnabrugge RL, Mylotte D, Head SJ, Van Mieghem NM, Nkomo VT, LeReun CM, et al. Aortic stenosis in the elderly: disease prevalence and number of candidates for transcatheter aortic valve replacement: a meta-analysis and modeling study. *J Am Coll Cardiol* 2013;**62**:1002–1012.

20. Attia ZI, Lerman G, Friedman PA. Deep neural networks learn by using human-selected electrocardiogram features and novel features. *Eur Heart J Digit Health* 2021;**2**:446–455.
21. Briand M, Dumesnil JG, Kadem L, Tongue AG, Rieu R, Garcia D, et al. Reduced systemic arterial compliance impacts significantly on left ventricular afterload and function in aortic stenosis: implications for diagnosis and treatment. *J Am Coll Cardiol* 2005;**46**:291–298.
22. Sutton-Tyrrell K, Newman A, Simonsick EM, Havlik R, Pahor M, Lakatta E, et al. Aortic stiffness is associated with visceral adiposity in older adults enrolled in the study of health, aging, and body composition. *Hypertension* 2001;**38**:429–433.
23. Park SJ, Enriquez-Sarano M, Chang SA, Choi JO, Lee SC, Park SW, et al. Hemodynamic patterns for symptomatic presentations of severe aortic stenosis. *JACC Cardiovasc Imaging* 2013;**6**:137–146.
24. Biner S, Rafique AM, Goykhman P, Morrissey RP, Naghi J, Siegel RJ. Prognostic value of E/E' ratio in patients with unoperated severe aortic stenosis. *JACC Cardiovasc Imaging* 2010;**3**:899–907.
25. Dahl JS, Barros-Gomes S, Videbaek L, Poulsen MK, Issa IF, Carter-Storch R, et al. Early diastolic strain rate in relation to systolic and diastolic function and prognosis in aortic stenosis. *JACC Cardiovasc Imaging* 2016;**9**:519–528.
26. Villari B, Campbell SE, Hess OM, Mall G, Vassalli G, Weber KT, et al. Influence of collagen network on left ventricular systolic and diastolic function in aortic valve disease. *J Am Coll Cardiol* 1993;**22**:1477–1484.
27. Hess OM, Villari B, Kraysenbuehl HP. Diastolic dysfunction in aortic stenosis. *Circulation* 1993;**87**:IV73–IV76.
28. Sasayama S, Ross J Jr, Franklin D, Bloor CM, Bishop S, Dilley RB. Adaptations of the left ventricle to chronic pressure overload. *Circ Res* 1976;**38**:172–178.
29. Herrmann S, Fries B, Liu D, Hu K, Stoerk S, Voelker W, et al. Differences in natural history of low- and high-gradient aortic stenosis from nonsevere to severe stage of the disease. *J Am Soc Echocardiogr* 2015;**28**:1270–1282.
30. Carabello BA, Paulus WJ. Aortic stenosis. *Lancet* 2009;**373**:956–966.
31. Rassi AN, Pibarot P, Elmariah S. Left ventricular remodelling in aortic stenosis. *Can J Cardiol* 2014;**30**:1004–1011.
32. Ito S, Miranda WR, Nkomo VT, Connolly HM, Pislaru SV, Greason KL, et al. Reduced left ventricular ejection fraction in patients with aortic stenosis. *J Am Coll Cardiol* 2018;**71**:1313–1321.
33. Clavel MA, Dumesnil JG, Capoulade R, Mathieu P, Senechal M, Pibarot P. Outcome of patients with aortic stenosis, small valve area, and low-flow, low-gradient despite preserved left ventricular ejection fraction. *J Am Coll Cardiol* 2012;**60**:1259–1267.
34. Eleid MF, Sorajja P, Michelena HI, Malouf JF, Scott CG, Pellikka PA. Survival by stroke volume index in patients with low-gradient normal EF severe aortic stenosis. *Heart* 2015;**101**:23–29.
35. Ito S, Miranda WR, Nkomo VT, Lewis BR, Oh JK. Sex differences in LV remodeling and hemodynamics in aortic stenosis: sex-specific criteria for severe stenosis? *JACC Cardiovasc Imaging* 2022;**15**:1175–1189.
36. Attia ZI, Kapa S, Lopez-Jimenez F, McKie PM, Ladewig DJ, Satam G, et al. Screening for cardiac contractile dysfunction using an artificial intelligence-enabled electrocardiogram. *Nat Med* 2019;**25**:70–74.
37. Attia ZI, Friedman PA, Noseworthy PA, Lopez-Jimenez F, Ladewig DJ, Satam G, et al. Age and sex estimation using artificial intelligence from standard 12-lead ECGs. *Circ Arrhythm Electrophysiol* 2019;**12**:e007284.
38. Attia ZI, Noseworthy PA, Lopez-Jimenez F, Asirvatham SJ, Deshmukh AJ, Gersh BJ, et al. An artificial intelligence-enabled ECG algorithm for the identification of patients with atrial fibrillation during sinus rhythm: a retrospective analysis of outcome prediction. *Lancet* 2019;**394**:861–867.
39. Ko WY, Siontis KC, Attia ZI, Carter RE, Kapa S, Ommen SR, et al. Detection of hypertrophic cardiomyopathy using a convolutional neural network-enabled electrocardiogram. *J Am Coll Cardiol* 2020;**75**:722–733.